


Precision measurement of the Λ_c^+ , Ξ_c^+ , and Ξ_c^0 baryon lifetimesR. Aaij *et al.**
(LHCb Collaboration) (Received 19 June 2019; published 1 August 2019)

We report measurements of the lifetimes of the Λ_c^+ , Ξ_c^+ and Ξ_c^0 charm baryons using proton-proton collision data at center-of-mass energies of 7 and 8 TeV, corresponding to an integrated luminosity of 3.0 fb^{-1} , collected by the LHCb experiment. The charm baryons are reconstructed through the decays $\Lambda_c^+ \rightarrow pK^-\pi^+$, $\Xi_c^+ \rightarrow pK^-\pi^+$ and $\Xi_c^0 \rightarrow pK^-K^-\pi^+$, and originate from semimuonic decays of beauty baryons. The lifetimes are measured relative to that of the D^+ meson, and are determined to be $\tau_{\Lambda_c^+} = 203.5 \pm 1.0 \pm 1.3 \pm 1.4 \text{ fs}$, $\tau_{\Xi_c^+} = 456.8 \pm 3.5 \pm 2.9 \pm 3.1 \text{ fs}$, $\tau_{\Xi_c^0} = 154.5 \pm 1.7 \pm 1.6 \pm 1.0 \text{ fs}$, where the uncertainties are statistical, systematic, and due to the uncertainty in the D^+ lifetime. The measurements are approximately 3–4 times more precise than the current world average values. The Λ_c^+ and Ξ_c^+ lifetimes are in agreement with previous measurements; however, the Ξ_c^0 baryon lifetime is approximately 3.3 standard deviations larger than the world average value.

DOI: [10.1103/PhysRevD.100.032001](https://doi.org/10.1103/PhysRevD.100.032001)

Measurements of the lifetimes of hadrons containing heavy (b or c) quarks play an important role in testing theoretical approaches that are used to perform Standard Model calculations. The validation of such tools is important, as they can then be used to search for deviations from Standard Model expectations in other processes. One of the most predictive tools in quark flavor physics is the heavy quark expansion (HQE) [1–7], which can be used to calculate the decay widths of hadrons containing heavy quarks, Q , through an expansion in inverse powers of the heavy quark mass, m_Q . The lowest-order term in the expansion depends only on m_Q , and therefore contributes equally to the decay width of all hadrons with a single heavy quark Q . Higher-order terms in the HQE are related to nonperturbative corrections, and to effects due to the presence of the other light (spectator) quark(s) in the heavy hadron. These corrections generally increase as the mass of the heavy quark decreases, and therefore measurements of charm-hadron lifetimes are sensitive to these higher-order contributions [8–13].

Particle lifetimes are also required to compare measured b - or c -hadron decay branching fractions to corresponding predictions for partial decay widths. Improved precision on the lifetimes thus allows for more stringent tests of

theoretical predictions. Lastly, improving the knowledge of the properties of all Standard Model particles is important, as they serve as input directly, or through simulation, into a wide variety of studies both within and beyond the Standard Model.

Recently, the LHCb collaboration reported a measurement of the Ω_c^0 lifetime [14] that was nearly four times larger than, and inconsistent with, the world average value. The lifetimes of the other three ground state singly charmed baryons (Λ_c^+ , Ξ_c^+ and Ξ_c^0) were last measured almost twenty years ago, and are only known with precisions of 3%, 6% and 10%, respectively [15]. The most precise measurements contributing to the average lifetimes are those from the FOCUS collaboration [16–18] based on signal sample sizes of approximately 8000 Λ_c^+ , 500 Ξ_c^+ and 100 Ξ_c^0 decays. For the Λ_c^+ baryon, there is mild tension between the average lifetime obtained from fixed target experiments [16,19,20] and that obtained by the CLEO collaboration [21].

The LHCb experiment has recorded samples of charm baryons that are larger than any previous sample by several orders of magnitude, through both prompt production and as secondary products of b -hadron decays. Given the large deviation seen in the recent Ω_c^0 lifetime measurement, the tension in the Λ_c^+ lifetime measurements, and the overall relatively poor precision on the Λ_c^+ , Ξ_c^+ and Ξ_c^0 lifetimes compared to those for the charm mesons, it is important to have additional precise measurements of the lifetimes of these baryons.

This paper reports new measurements of the lifetimes of the Λ_c^+ , Ξ_c^+ and Ξ_c^0 baryons using samples of semileptonic $\Lambda_b^0 \rightarrow \Lambda_c^+\mu^-\bar{\nu}_\mu X$, $\Xi_b^0 \rightarrow \Xi_c^+\mu^-\bar{\nu}_\mu X$, and $\Xi_b^- \rightarrow \Xi_c^0\mu^-\bar{\nu}_\mu X$

*Full author list given at the end of the article.

Published by the American Physical Society under the terms of the [Creative Commons Attribution 4.0 International license](https://creativecommons.org/licenses/by/4.0/). Further distribution of this work must maintain attribution to the author(s) and the published article's title, journal citation, and DOI. Funded by SCOAP³.

decays, respectively.¹ The symbol X represents any additional undetected particles. The Λ_c^+ and Ξ_c^+ baryons are both reconstructed in the $pK^-\pi^+$ final state and the Ξ_c^0 baryon is observed through its decay to $pK^-K^-\pi^+$. The technique employed to measure the charm-baryon lifetimes follows that used to measure the Ω_c^0 lifetime in Ref. [14].

To reduce the uncertainties associated with systematic effects, the lifetime ratio

$$r_{H_c} \equiv \frac{\tau_{H_c}}{\tau_{D^+}} \quad (1)$$

is measured, where the D^+ meson is reconstructed using $B \rightarrow D^+\mu^-\bar{\nu}_\mu X$ decays, with $D^+ \rightarrow K^-\pi^+\pi^+$. The symbols H_b and H_c are used here and throughout to refer to the b or c hadron in any of the modes indicated above.

The measurements presented in this paper use proton-proton (pp) collision data samples collected by the LHCb experiment, corresponding to an integrated luminosity of 3.0 fb^{-1} , of which 1.0 fb^{-1} was recorded at a center-of-mass energy of 7 TeV and 2.0 fb^{-1} at 8 TeV. The LHCb detector [22,23] is a single-arm forward spectrometer covering the pseudorapidity range $2 < \eta < 5$, designed for the study of particles containing b or c quarks. The tracking system provides a measurement of the momentum, p , of charged particles with a relative uncertainty that varies from 0.5% at low momentum to 1.0% at 200 GeV/ c . The minimum distance of a track to a primary vertex (PV), the impact parameter (IP), is measured with a resolution of $\sigma_{\text{IP}} = (15 + 29/p_T) \mu\text{m}$ [24], where p_T is the component of the momentum transverse to the beam, in GeV/ c . Charged hadrons are identified using information from two ring-imaging Cherenkov (RICH) detectors [25]. Muons are identified by a system composed of alternating layers of iron and multiwire proportional chambers [26]. The online event selection is performed by a trigger [27], which consists of a hardware stage, based on information from the calorimeter and muon systems, followed by a software stage, which applies a full event reconstruction.

Simulation is required to model the effects of the detector acceptance and resolution, as well as the imposed selection requirements. Proton-proton collisions are simulated using PYTHIA [28] with a specific LHCb configuration [29]. Decays of hadronic particles are described by EVTGEN [30], in which final-state radiation is generated using PHOTOS [31]. The interaction of the generated particles with the detector and its response are implemented using the GEANT4 toolkit [32] as described in Ref. [33].

Samples of candidate semileptonic H_b decays are formed by combining a μ^- candidate with a charm-hadron candidate, reconstructed through one of the following modes: $\Lambda_c^+ \rightarrow pK^-\pi^+$, $\Xi_c^+ \rightarrow pK^-\pi^+$, $\Xi_c^0 \rightarrow pK^-K^-\pi^+$,

or $D^+ \rightarrow K^-\pi^+\pi^+$. All final-state charged particles are required to be detached from all PVs in the event. This selection is based upon a quantity χ_{IP}^2 , which is the difference in the χ^2 of the PV fit with and without the inclusion of the particle under consideration. The requirement on χ_{IP}^2 for the p , K^- and π^+ (μ^-) candidates corresponds to about $2\sigma_{\text{IP}}$ ($3\sigma_{\text{IP}}$). The muon is required to have $p_T > 1 \text{ GeV}/c$, $p > 6 \text{ GeV}/c$ and have particle identification (PID) information consistent with that of a muon. The final-state hadrons must have PID information consistent with their assumed particle hypotheses, and have $p_T > 0.25 \text{ GeV}/c$ and $p > 2 \text{ GeV}/c$. To remove the contribution from promptly produced charm baryons, the reconstructed trajectory of the H_c candidate must not point back to any PV in the event. Only H_c candidates that have an invariant mass within $60 \text{ MeV}/c^2$ of their known mass are retained.

The $H_c\mu^-$ combinations are required to form a good quality vertex and satisfy the invariant mass requirement, $m(H_c\mu^-) < 8.0 \text{ GeV}/c^2$. Random combinations of H_c and μ^- are suppressed by requiring the H_c decay vertex to be downstream of the reconstructed $H_c\mu^-$ decay vertex. In events with more than one PV, the b -hadron candidate and its decay products are associated to the PV for which the χ_{IP}^2 of the b hadron is smallest.

The dominant source of background in the $H_b \rightarrow H_c\mu^-$ samples is from other semileptonic b -hadron decays. To suppress the background in the Λ_c^+ and Ξ_c^+ samples from misidentified $D_s^+ \rightarrow K^+K^-\pi^+$, $D^+ \rightarrow K^-\pi^+\pi^+$, $D^{*+} \rightarrow D^0(\rightarrow K^-\pi^+)\pi^+$, and $D \rightarrow \phi(\rightarrow K^+K^-)X$ decays, a set of vetoes is employed. The vetoes are only applied to candidates that have an invariant mass consistent (within ~ 2.5 times the mass resolution) with either the known D_s^+ mass, D^+ mass, the $D^{*+} - D^0$ mass difference, or the ϕ meson mass, after substituting either the kaon or pion mass in place of the proton mass in the reconstructed decay chain. For those candidates, tighter PID requirements are imposed such that any peaking contribution is removed. The veto removes about 1%–2% of the signal, and reduces the total background by about 15% (25%) in the Λ_c^+ (Ξ_c^+) samples. Potential contamination in the Ξ_c^0 sample from fully reconstructed, but misidentified, four-body D^0 meson decays has been investigated, and is found to be negligible. After all selections, the dominant source of background is from real muons combined with partially reconstructed or misidentified charm-hadron decays.

After applying the above selections, the Ξ_c^+ sample still has a lower signal-to-background ratio than the Λ_c^+ and Ξ_c^0 samples. To improve the signal-to-background ratio in the $\Xi_c^+\mu^-$ sample, a boosted decision tree (BDT) discriminant [34,35] is built from 18 variables. The variables are the χ^2 for the Ξ_c^0 and Ξ_c^+ decay-vertex fits, and for each final-state hadron: p , p_T , χ_{IP}^2 to the associated PV, and a PID response variable. The BDT is trained using simulated

¹Throughout the text, charge-conjugate processes are implicitly included.

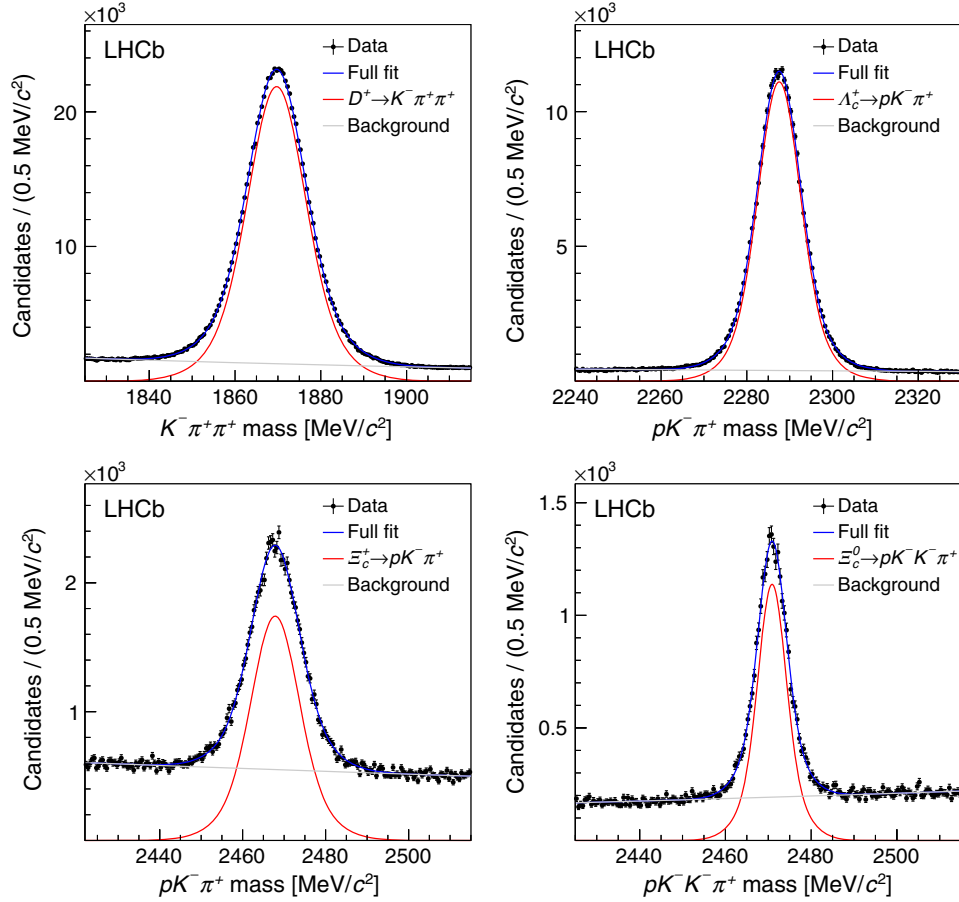


FIG. 1. Invariant-mass distributions for candidate (top left) D^+ in $B \rightarrow D^+ \mu^- \bar{\nu}_\mu X$, (top right) Λ_c^+ in $\Lambda_b^0 \rightarrow \Lambda_c^+ \mu^- \bar{\nu}_\mu X$, (bottom left) Ξ_c^+ in $\Xi_b^0 \rightarrow \Xi_c^+ \mu^- \bar{\nu}_\mu X$, and (bottom right) Ξ_c^0 in $\Xi_b^- \rightarrow \Xi_c^0 \mu^- \bar{\nu}_\mu X$ candidate decays. The results of the fits, as described in the text, are overlaid.

$\Xi_b^0 \rightarrow \Xi_c^+ \mu^- \bar{\nu}_\mu X$ decays for the signal, while background is taken from the Ξ_c^+ mass sidebands, $30 < |m(pK^- \pi^+) - m_{\Xi_c^+}| < 50 \text{ MeV}/c^2$, where $m_{\Xi_c^+}$ is the known Ξ_c^+ mass [15]. Only a loose requirement on the BDT is employed, which provides an efficiency of about 97% for signal decays while suppressing 40% of the background.

Signal candidates must satisfy a well-defined set of hardware and software trigger requirements. At the hardware level, signal candidates are required to include a high p_T muon. At the software level, they must pass a topological multivariate selection designed to provide an enriched sample of beauty hadrons decaying to multibody final states containing a muon [36].

The invariant-mass distributions for the selected D^+ , Λ_c^+ , Ξ_c^+ and Ξ_c^0 candidates in the $H_c \mu^-$ final states are shown in Fig. 1. For the Λ_c^+ and D^+ samples only a 10% randomly selected subsample of events is used in this analysis, since the full yield is much larger than is needed in this analysis given the anticipated size of the systematic uncertainties. A binned maximum-likelihood fit is performed to each of the four samples to obtain the signal yields. For each mass distribution, the signal shape is parametrized as the sum of

two Gaussian functions with a common mean, and the background shape is described using an exponential function. All signal and background shape parameters are freely varied in the fit. The resulting signal yields are given in Table I. The Ξ_c^+ and Ξ_c^0 yields are about 100 times larger than any previous sample used to measure the lifetimes of these baryons, and the Λ_c^+ sample is about 40 times larger.

The decay time of each H_c candidate is determined from the positions of the H_b and H_c decay vertices, and the

TABLE I. Yields from the binned maximum-likelihood fits to the H_c invariant mass spectra in $H_c \mu^-$ signal candidates. For the Λ_c^+ and D^+ modes, only 10% of the sample is used, since the yields in the full dataset are much larger than needed in this analysis.

H_c	Yield (10^3)
D^+	809.4 ± 1.3
Λ_c^+	303.5 ± 0.7
Ξ_c^+	55.8 ± 0.5
Ξ_c^0	21.6 ± 0.2

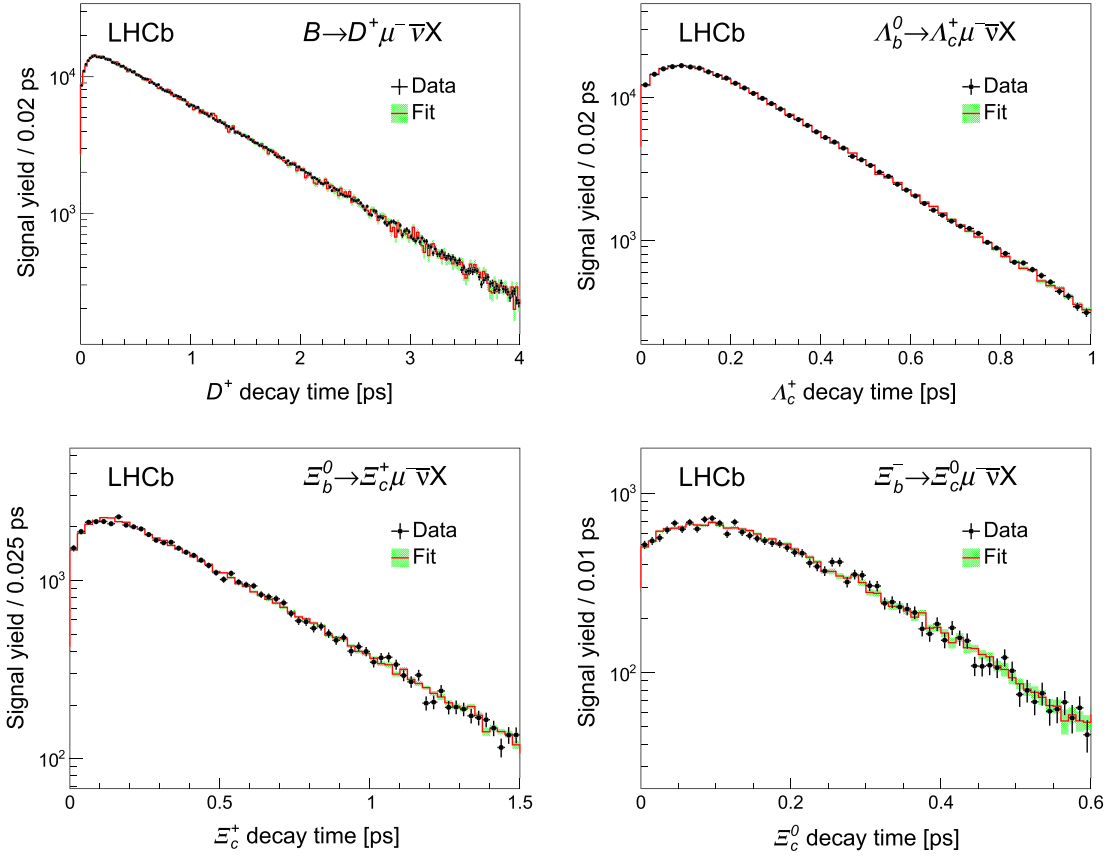


FIG. 2. Decay-time spectra for (top left) D^+ signal in $B \rightarrow D^+ \mu^- \bar{\nu}_\mu X$, (top right) Λ_c^+ signal in $\Lambda_b^0 \rightarrow \Lambda_c^+ \mu^- \bar{\nu}_\mu X$, (bottom left) Ξ_c^+ signal in $\Xi_b^0 \rightarrow \Xi_c^+ \mu^- \bar{\nu}_\mu X$, and (bottom right) Ξ_c^0 signal in $\Xi_b^- \rightarrow \Xi_c^0 \mu^- \bar{\nu}_\mu X$ candidate decays. Overlaid are the fit results, as described in the text, along with the uncertainties due to finite sizes of the simulated samples.

measured H_c momentum. Because b hadrons have a mean lifetime of about 1.5 ps, the decay vertices are well separated from the PV. As a result, systematic effects due to lifetime-biasing selections in the trigger or offline analysis are greatly reduced compared to promptly produced charmed baryons.

The background-subtracted decay-time spectra are obtained using the *sPlot* technique [37], where the measured H_c mass is used as the discriminating variable. To improve the accuracy of the *sPlot* background subtraction, a correction to the H_c mass is applied to remove a small dependence of the mean reconstructed H_c mass on its reconstructed decay time, t_{rec} . This correction is obtained by first fitting for the peak position of the reconstructed mass, $M_{\text{peak}}^{H_c}(t_{\text{rec}})$, in bins of reconstructed decay time, followed by a fit for the dependence of $M_{\text{peak}}^{H_c}(t_{\text{rec}})$ on t_{rec} , using the functional form

$$M^{H_c}(0) + A[1 - \exp(-t_{\text{rec}}/C)]. \quad (2)$$

The second term represents the deviation from a constant value, and is used to correct the measured H_c mass of every candidate used in the *sPlot*. For the four modes under study,

the values of A and C range from 2.7–4.1 MeV/ c^2 and 0.06–0.17 ps, respectively. The uncertainties in the signal yields reflect both the finite signal yield and the statistical uncertainty associated with the background subtraction.

Potential backgrounds from random $H_c \mu^-$ combinations, where the muon is not produced directly at the H_b decay vertex, could lead to a bias on the lifetime. Such decays include $H_b \rightarrow H_c \tau^- \bar{\nu}_\tau$, $\tau^- \rightarrow \mu^- \nu_\tau \bar{\nu}_\mu$ and $H_b \rightarrow H_c \bar{D}$, $\bar{D} \rightarrow \mu^- X$, where \bar{D} represents a D_s^- , D^- or \bar{D}^0 meson. These backgrounds are a small fraction of the observed signal, about 3% in total, and have decay-time spectra that are similar to the genuine $H_c \mu^- \bar{\nu}_\mu$ final state due to the χ^2 requirements on the H_b vertex fit. The effect of these backgrounds is studied with simulation and pseudoexperiments, and is included as a source of systematic uncertainty.

The decay-time spectra for the D^+ , Λ_c^+ , Ξ_c^+ and Ξ_c^0 signals are shown in Fig. 2, along with the results of the fits described below. Only H_c candidates with decay time larger than zero are used in the fit. The decrease in signal yield as the decay time approaches zero is mainly due to the H_c decay-time resolution, typically in the 85–100 fs range, which results in migration of the signal into the negative decay-time region.

The charm-hadron lifetimes are determined by fitting the decay-time spectra using a binned χ^2 fit over the ranges shown in Fig. 2. The signal decay-time model takes the form

$$S(t_{\text{rec}}; \tau_{\text{sim}}^{H_c}) = f(t_{\text{rec}}; \tau_{\text{sim}}^{H_c})g(t_{\text{rec}})\beta(t_{\text{rec}}), \quad (3)$$

where $f(t_{\text{rec}}; \tau_{\text{sim}}^{H_c})$ is a signal template of reconstructed decay times obtained from the full LHCb simulation with input lifetime $\tau_{\text{sim}}^{H_c}$. The selection requirements applied to the simulation are identical to those applied to the data. The function

$$g(t_{\text{rec}}) = \exp(-t_{\text{rec}}/\tau_{\text{fit}}^{H_c}) / \exp(-t_{\text{rec}}/\tau_{\text{sim}}^{H_c}) \quad (4)$$

weights the simulated template with lifetime $\tau_{\text{sim}}^{H_c}$ to a lifetime value $\tau_{\text{fit}}^{H_c}$. Because the weighting function $g(t_{\text{rec}})$ depends on the reconstructed decay time, t_{rec} , rather than the true decay time, there is a dependence of $S(t_{\text{rec}}; \tau_{\text{sim}}^{H_c})$ on the $\tau_{\text{sim}}^{H_c}$ value used to generate the template. The simulation uses the known D^+ lifetime, $\tau_{\text{sim}}^{D^+} = 1040$ fs, which is accurately measured by many experiments [15]. Since the charm-baryon lifetimes in this analysis are expected to have a better precision than the existing world average values, a number of different $\tau_{\text{sim}}^{H_c}$ templates are produced. An optimization procedure, as described below, is used to determine the best choice of $\tau_{\text{sim}}^{H_c}$ to use for the charm-baryon templates. The simulation includes contributions from $H_c\tau^-\bar{\nu}_c X$ final states as well as excited charm hadrons.

The function $\beta(t_{\text{rec}})$ corrects for a small difference in the efficiency between data and simulation for reconstructing tracks in the vertex detector that originate far from the beamline [38]. As discussed in Ref. [14], $\beta(t)$ is calibrated using the precisely known value of the D^+ lifetime, from which it is found that $\beta(t_{\text{rec}}) = 1 + \beta_0 t_{\text{rec}}$, with $\beta_0 = (-0.89 \pm 0.32) \times 10^{-2} \text{ ps}^{-1}$. The result of the binned χ^2 fit to the D^+ decay-time spectrum after this correction is applied is shown in Fig. 2 (top left), where the fitted lifetime is found to be $\tau_{\text{fit}}^{D^+} = 1042.0 \pm 1.7(\text{stat})$ fs. The inclusion of the $\beta(t)$ term in $S(t_{\text{rec}})$ amounts to about a 1% positive correction to the measured lifetime.

Since beauty baryonic decays are not perfectly described by the simulation, the simulated events are weighted in bins of (p_T, η) of the beauty baryon and the mass $m(H_c\mu^-)$ of the $H_c\mu^-$ system to match that which is observed in background-subtracted data. The simulation is also weighted to match all of the two-body invariant mass projections among the H_c decay products. After all of these weights are applied, excellent agreement is seen for a wide range of observables in these decays, most notably those that are used in the BDT. These weights are applied in the formation of the $f(t_{\text{rec}}; \tau_{\text{sim}}^{H_c})$ templates.

The lifetime of each charmed baryon is determined from a simultaneous fit to its decay-time spectrum and that of the D^+ meson. In these fits, $\tau_{\text{fit}}^{H_c}$ in Eq. (4) is replaced by $r_{H_c} \tau_{\text{fit}}^{D^+}$ in order to reduce systematic uncertainties. Thus, the free parameters in the fit are r_{H_c} , as shown in Eq. (1), and $\tau_{\text{fit}}^{D^+}$. In the Ξ_c^0 decay-time fit, β_0 is scaled by 4/3 since the effect scales with the number of charged final-state particles in the H_c decay [38].

The procedure for determining the optimal values of $\tau_{\text{sim}}^{H_c}$ to use in forming the templates $f(t_{\text{rec}}; \tau_{\text{sim}}^{H_c})$ is first developed and validated using simulation. A series of templates, $f_i(t_{\text{rec}}; \tau_{\text{sim}}^{H_c})$, spanning a wide range of $\tau_{\text{sim}}^{H_c}$ values is produced for each charm baryon. From one template with true lifetime $\tau_{\text{sim}}^{H_c, \text{true}}$, a pseudodataset set of decay times is formed that has comparable yield to that of the data. The decay-time fit is then performed using each template $f_i(t_{\text{rec}}; \tau_{\text{sim}}^{H_c})$ to this pseudodataset, with each fit yielding a value of τ_{fit} and a χ^2 of the fit. Examination of the results show, as expected, that when the pseudodataset are fit using the correct template, τ_{fit} is consistent with $\tau_{\text{sim}}^{H_c, \text{true}}$. Conversely, when the same pseudodataset is fit with an alternate template that is produced with a significantly different input value of $\tau_{\text{sim}}^{H_c}$, τ_{fit} deviates from $\tau_{\text{sim}}^{H_c, \text{true}}$. Thus the criterion for choosing the optimal template is to select that in which τ_{fit} is closest to $\tau_{\text{sim}}^{H_c}$. The chosen template is also found to have the lowest fit χ^2 , which provides additional support for the method of determining the optimal template.

Applying this same criterion to the data, the optimal values of $\tau_{\text{sim}}^{H_c}$ are found to be $\tau_{\text{sim}}^{\Lambda_c^+} = 203$ fs, $\tau_{\text{sim}}^{\Xi_c^+} = 455$ fs, and $\tau_{\text{sim}}^{\Xi_c^0} = 155$ fs. As with the pseudodata, these optimal values also yield the lowest χ^2 value for the decay-time fit. Slightly different values of $\tau_{\text{sim}}^{H_c}$ are not excluded by the procedure, and are considered as a source of systematic uncertainty.

The results of the fits to the Λ_c^+ , Ξ_c^+ and Ξ_c^0 decay-time distributions using the best-fit templates are shown in Fig. 2 and corresponds to the ratios

$$r_{\Lambda_c^+} = 0.1956 \pm 0.0010,$$

$$r_{\Xi_c^+} = 0.4392 \pm 0.0034,$$

$$r_{\Xi_c^0} = 0.1485 \pm 0.0017,$$

where the uncertainties are statistical only. Multiplying these ratios by the D^+ lifetime [15], leads to the lifetimes

$$\tau_{\Lambda_c^+} = 203.5 \pm 1.0 \text{ fs},$$

$$\tau_{\Xi_c^+} = 456.8 \pm 3.5 \text{ fs},$$

$$\tau_{\Xi_c^0} = 154.5 \pm 1.7 \text{ fs}.$$

TABLE II. Summary of systematic uncertainties on the ratio of the charm baryon to D^+ meson lifetimes (in units of 10^{-4}). The statistical uncertainty on the measurements is also provided for reference.

Source	$r_{\Lambda_c^+}$	$r_{\Xi_c^+}$	$r_{\Xi_c^0}$
Decay-time acceptance	6	13	4
H_c lifetime	4	4	12
H_b lifetime	1	3	0
H_b production spectra	2	4	1
Background subtraction	8	17	7
$H_c(\tau^-, D, \text{random } \mu^-)$	5	11	3
Simulated sample size	4	13	5
Total systematic	13	28	16
Statistical uncertainty	10	34	17

The statistical precision of these measurements is 5–8 times better than those of the current world average values [15].

A number of sources of systematic uncertainty on the measured ratios r_{H_c} are summarized in Table II. The decay-time acceptance correction, $\beta(t_{\text{rec}})$, leads to an uncertainty of 0.5% on r_{H_c} . This uncertainty includes a contribution from the finite $B \rightarrow D^+ \mu^- X$ sample sizes and the choice of fit function.

The technique for finding the correct template is based on choosing that in which the fitted lifetime is most consistent with the value used in the simulation. The uncertainty due to this choice is estimated by repeating the decay-time fit using alternative templates that have simulated lifetimes that differ from the nominal one by two times the uncertainty on the fitted lifetime. The difference between the fitted values of r_{H_c} for these alternative templates and the nominal one is assigned as a systematic uncertainty.

The Λ_b^0 , Ξ_b^0 and Ξ_b^- lifetimes are not known precisely, and this has a small effect on the decay-time acceptance. To study this effect, simulated decays are weighted to produce either a shorter or longer H_b lifetime, based on the known uncertainties on the b -baryon lifetimes [15]. New signal templates are formed, and the fits are repeated. The change in the fitted value of r_{H_c} is assigned as a systematic uncertainty.

Studies of the D^+ calibration mode show a small difference in the reconstruction efficiency between data and simulation, which is described by the β_0 parameter. This parameter has a small dependence on the p_T and η of the H_b hadron. While the signal mode simulations are weighted to match the (p_T, η) spectrum observed in data, the weighting is imperfect. A difference would lead to a small bias in the average value of β_0 . The uncertainty on r_{H_c} is obtained by taking into account the variation of β_0 in different p_T and η ranges, and the extent to which the (p_T, η) spectrum differs between data and simulation for each of the decay modes.

The decay-time resolution is checked by comparing the D^0 decay-time spectra in $B^- \rightarrow D^0 \pi^-$ decays between data and simulation, where no explicit requirement on the D^0 flight distance is applied. The simulation reproduces the data well. A second check is performed where the Λ_c^+ lifetime is fitted using a template that is produced with an additional smearing which increases the decay-time resolution by 2.5%. The change increases the fit χ^2 substantially, with only a small change of 0.3 fs in the fitted lifetime. This difference is considered negligible, and no systematic uncertainty due to modeling the decay-time resolution is assigned.

The method for background subtraction uses the *sPlot* technique, which relies on a specific choice for modeling the signal and background distributions in the charm-hadron invariant-mass spectra. To quantify a possible systematic effect on r_{H_c} , the decay-time spectra in data are obtained using a different background-subtraction technique. Instead of the *sPlot* method, signal and sideband regions are defined for each of the mass spectra, and for each charm baryon the decay-time spectrum of candidates from the sideband regions are subtracted from the spectrum obtained from the signal region. The resulting background-subtracted decay-time spectra are then fitted using the decay-time fit described previously. The difference between this result and the nominal one is assigned as a systematic uncertainty.

The decay-time spectra in the $H_c \mu^-$ samples have small contributions from random combinations of H_c and μ^- candidates [(0.8 ± 0.2)% of the signal], as well as backgrounds where the muon comes from either a τ^- [(1.8 ± 0.3)%] or a semileptonic D decay [(0.5 ± 0.2)%]. The impact of these backgrounds is assessed using pseudoexperiments, as described in Ref. [14].

The systematic uncertainty due to the finite size of the simulated samples used to produce the signal templates is assessed by repeating the fit to the data many times, where in each fit the simulated-template bin contents are fluctuated within their uncertainties. The standard deviation of the distribution of the fitted r_{H_c} values is assigned as a systematic uncertainty. The total systematic uncertainty on r_{H_c} is about 0.6% for the Λ_c^+ and Ξ_c^+ measurements, and about 1.2% for that of the Ξ_c^0 baryon.

In summary, pp collision data samples at 7 TeV and 8 TeV center-of-mass energies collected by the LHCb experiment, corresponding to 3.0 fb⁻¹ of integrated luminosity, are used to measure the lifetimes of the Λ_c^+ , Ξ_c^+ and Ξ_c^0 baryons. For the Λ_c^+ and D^+ samples, only 10% of the integrated luminosity is used for this measurement. The lifetimes, measured relative to that of the D^+ meson, are determined to be

$$r_{\Lambda_c^+} = 0.1956 \pm 0.0010 \pm 0.0013,$$

$$r_{\Xi_c^+} = 0.4392 \pm 0.0034 \pm 0.0028,$$

$$r_{\Xi_c^0} = 0.1485 \pm 0.0017 \pm 0.0016,$$

where the first uncertainty is statistical and the second is systematic. After multiplying by the known D^+ lifetime of 1040 ± 7 fs [15], the charm-baryon lifetimes are measured to be

$$\tau_{\Lambda_c^+} = 203.5 \pm 1.0 \pm 1.3 \pm 1.4 \text{ fs,}$$

$$\tau_{\Xi_c^+} = 456.8 \pm 3.5 \pm 2.9 \pm 3.1 \text{ fs,}$$

$$\tau_{\Xi_c^0} = 154.5 \pm 1.7 \pm 1.6 \pm 1.0 \text{ fs,}$$

where the last uncertainty is due to the uncertainty in the D^+ lifetime. The Λ_c^+ and Ξ_c^+ lifetimes are measured with about 1% precision and are consistent with the existing world averages. The Ξ_c^0 lifetime is measured with about 1.8% precision, and is 3.3σ larger than the world average value of 112_{-10}^{+13} fs. These measurements have uncertainties that are approximately 3–4 times smaller than those of the existing world average values, and have precision comparable to that achieved for charm mesons.

We express our gratitude to our colleagues in the CERN accelerator departments for the excellent performance of the LHC. We thank the technical and administrative staff at the LHCb institutes. We acknowledge support from CERN and from the national agencies: CAPES, CNPq, FAPERJ and FINEP (Brazil); MOST and NSFC (China); CNRS/IN2P3 (France); BMBF, DFG and MPG (Germany); INFN (Italy);

NWO (Netherlands); MNiSW and NCN (Poland); Institut de Fizica Atomica (Romania); Ministry of Education and Science of the Russian Federation (Russia); MinECo (Spain); SNSF and State Secretariat for Education, Research and Innovation (Switzerland); NASU (Ukraine); STFC (United Kingdom); DOE NP and NSF (USA). We acknowledge the computing resources that are provided by CERN, IN2P3 (France), KIT and DESY (Germany), INFN (Italy), SURF (Netherlands), PIC (Spain), GridPP (United Kingdom), RRCKI and Yandex LLC (Russia), CSCS (Switzerland), IFIN-HH (Romania), CBPF (Brazil), PL-GRID (Poland) and OSC (USA). We are indebted to the communities behind the multiple open-source software packages on which we depend. Individual groups or members have received support from AvH Foundation (Germany); EPLANET, Marie Skłodowska-Curie Actions and ERC (European Union); ANR, Labex P2IO and Labex OCEVU, Origine Constituants et Evolution de l'Univers, and Région Auvergne-Rhône-Alpes (France); Key Research Program of Frontier Sciences of CAS, CAS PIFI, and the Thousand Talents Program (China); RFBR, RSF and Yandex LLC (Russia); Generalitat Valenciana, the regional government of Valencia, in Spain, XuntaGal and Generalitat de Catalunya (Spain); the Royal Society and the Leverhulme Trust (United Kingdom).

-
- [1] V. A. Khoze and M. A. Shifman, Heavy quarks, *Sov. Phys. Usp.* **26**, 387 (1983).
- [2] I. I. Bigi and N. G. Uraltsev, Gluonic enhancements in non-spectator beauty decays—an inclusive mirage though an exclusive possibility, *Phys. Lett. B* **280**, 271 (1992).
- [3] I. I. Bigi, N. G. Uraltsev, and A. I. Vainshtein, Nonperturbative corrections to inclusive beauty and charm decays. QCD versus phenomenological models, *Phys. Lett. B* **293**, 430 (1992), Erratum **297**, 477 (1992).
- [4] B. Blok and M. Shifman, The rule of discarding $1/N_c$ in inclusive weak decays (I), *Nucl. Phys.* **B399**, 441 (1993); The rule of discarding $1/N_c$ in inclusive weak decays (II), *Nucl. Phys.* **B399**, 459 (1993).
- [5] M. Neubert, B decays and the heavy-quark expansion, *Adv. Ser. Dir. High Energy Phys.* **15**, 239 (1998).
- [6] N. Uraltsev, Heavy quark expansion in beauty and its decays, *Proceedings of the International School of Physics “Enrico Fermi”* **137**, 329 (1998), also published in *Proceedings of the Heavy Flavour Physics: A Probe of Nature’s Grand Design, Proceedings, International School of Physics “Enrico Fermi”, Course CXXXVII, Varenna* (IOS Press, Amsterdam, 1997).
- [7] I. I. Bigi, The QCD perspective on lifetimes of heavy-flavour hadrons, [arXiv:hep-ph/9508408](https://arxiv.org/abs/hep-ph/9508408).
- [8] M. Kirk, A. Lenz, and T. Rauh, Dimension-six matrix elements for meson mixing and lifetimes from sum rules, *J. High Energy Phys.* **12** (2017) 068.
- [9] H.-Y. Cheng, Charmed baryons circa 2015, *Front. Phys.* **10**, 101406 (2015); Strong decays of charmed baryons in heavy hadron chiral perturbation theory: An update, *Phys. Rev. D* **92**, 074014 (2015).
- [10] A. Lenz and T. Rauh, D-meson lifetimes within the heavy quark expansion, *Phys. Rev. D* **88**, 034004 (2013).
- [11] S. Bianco, F. L. Fabbri, D. Benson, and I. I. Bigi, A cicerone for the physics of charm, *Riv. Nuovo Cimento* **26N7**, 1 (2003).
- [12] G. Bellini, I. I. Bigi, and P. J. Dornan, Lifetimes of charm and beauty hadrons, *Phys. Rep.* **289**, 1 (1997).
- [13] B. Blok and M. A. Shifman, Lifetimes of charmed hadrons revisited. Facts and fancy, in *Tau charm factory, Proceedings of the 3rd Workshop, Marbella, Spain, 1993* (Editions Frontieres, Gif-Sur-Yvette, 1991); Reports No. Technion-PH-93-41, No. TPI-MINN-93/55-T.
- [14] R. Aaij *et al.* (LHCb Collaboration), Measurement of the Ω_c^0 Baryon Lifetime, *Phys. Rev. Lett.* **121**, 092003 (2018).
- [15] M. Tanabashi *et al.* (Particle Data Group), Review of particle physics, *Phys. Rev. D* **98**, 030001 (2018).
- [16] J. M. Link *et al.* (FOCUS Collaboration), A High Statistics Measurement of the Λ_c^+ Lifetime, *Phys. Rev. Lett.* **88**, 161801 (2002).

- [17] J. M. Link *et al.* (FOCUS Collaboration), A new measurement of the Ξ_c^+ lifetime, *Phys. Lett. B* **523**, 53 (2001).
- [18] J. M. Link *et al.* (FOCUS Collaboration), A new measurement of the Ξ_c^0 lifetime, *Phys. Lett. B* **541**, 211 (2002).
- [19] A. Kushnirenko *et al.* (SELEX Collaboration), Precision Measurements of the Λ_c^+ and D^0 Lifetimes, *Phys. Rev. Lett.* **86**, 5243 (2001).
- [20] P. L. Frabetti *et al.* (E687 Collaboration), Measurement of the Λ_c^+ Lifetime, *Phys. Rev. Lett.* **70**, 1755 (1993).
- [21] A. H. Mahmood *et al.* (CLEO Collaboration), Measurement of the Λ_c^+ Lifetime, *Phys. Rev. Lett.* **86**, 2232 (2001).
- [22] A. A. Alves, Jr. *et al.* (LHCb Collaboration), The LHCb detector at the LHC, *J. Instrum.* **3**, S08005 (2008).
- [23] R. Aaij *et al.* (LHCb Collaboration), LHCb detector performance, *Int. J. Mod. Phys. A* **30**, 1530022 (2015).
- [24] R. Aaij *et al.*, Performance of the LHCb vertex locator, *J. Instrum.* **9**, P09007 (2014).
- [25] M. Adinolfi *et al.*, Performance of the LHCb RICH detector at the LHC, *Eur. Phys. J. C* **73**, 2431 (2013).
- [26] F. Archilli *et al.*, Performance of the muon identification at LHCb, *J. Instrum.* **8**, P10020 (2013).
- [27] R. Aaij *et al.*, The LHCb trigger and its performance in 2011, *J. Instrum.* **8**, P04022 (2013).
- [28] T. Sjöstrand, S. Mrenna, and P. Skands, PYTHIA 6.4 physics and manual, *J. High Energy Phys.* **05** (2006) 026; A brief introduction to PYTHIA 8.1, *Comput. Phys. Commun.* **178**, 852 (2008).
- [29] I. Belyaev *et al.*, Handling of the generation of primary events in Gauss, the LHCb simulation framework, *J. Phys. Conf. Ser.* **331**, 032047 (2011).
- [30] D. J. Lange, The EvtGen particle decay simulation package, *Nucl. Instrum. Methods Phys. Res., Sect. A* **462**, 152 (2001).
- [31] P. Golonka and Z. Was, PHOTOS Monte Carlo: A precision tool for QED corrections in Z and W decays, *Eur. Phys. J. C* **45**, 97 (2006).
- [32] J. Allison *et al.* (Geant4 Collaboration), Geant4 developments and applications, *IEEE Trans. Nucl. Sci.* **53**, 270 (2006); S. Agostinelli *et al.* (Geant4 Collaboration), Geant4: A simulation toolkit, *Nucl. Instrum. Methods Phys. Res., Sect. A* **506**, 250 (2003).
- [33] M. Clemencic, G. Corti, S. Easo, C. R. Jones, S. Miglioranza, M. Pappagallo, and P. Robbe *et al.*, The LHCb simulation application, Gauss: Design, evolution and experience, *J. Phys. Conf. Ser.* **331**, 032023 (2011).
- [34] L. Breiman, J. H. Friedman, R. A. Olshen, and C. J. Stone, *Classification and Regression Trees* (Wadsworth International Group, Belmont, California, 1984).
- [35] Y. Freund and R. E. Schapire, A decision-theoretic generalization of on-line learning and an application to boosting, *J. Comput. Syst. Sci.* **55**, 119 (1997).
- [36] V. V. Gligorov and M. Williams, Efficient, reliable and fast high-level triggering using a bonsai boosted decision tree, *J. Instrum.* **8**, P02013 (2013).
- [37] M. Pivk and F. R. Le Diberder, sPlot: A statistical tool to unfold data distributions, *Nucl. Instrum. Methods Phys. Res., Sect. A* **555**, 356 (2005).
- [38] R. Aaij *et al.* (LHCb Collaboration), Measurements of the B^+ , B^0 , B_s^0 meson and Λ_b^0 baryon lifetimes, *J. High Energy Phys.* **04** (2014) 114.

R. Aaij,²⁹ C. Abellán Beteta,⁴⁶ B. Adeva,⁴³ M. Adinolfi,⁵⁰ C. A. Aidala,⁷⁷ Z. Ajaltouni,⁷ S. Akar,⁶¹ P. Albicocco,²⁰ J. Albrecht,¹² F. Alessio,⁴⁴ M. Alexander,⁵⁵ A. Alfonso Alberro,⁴² G. Alkhazov,³⁵ P. Alvarez Cartelle,⁵⁷ A. A. Alves Jr.,⁴³ S. Amato,² Y. Amhis,⁹ L. An,¹⁹ L. Anderlini,¹⁹ G. Andreassi,⁴⁵ M. Andreotti,¹⁸ J. E. Andrews,⁶² F. Archilli,²⁹ J. Arnau Romeu,⁸ A. Artamonov,⁴¹ M. Artuso,⁶³ K. Arzymatov,³⁹ E. Aslanides,⁸ M. Atzeni,⁴⁶ B. Audurier,²⁴ S. Bachmann,¹⁴ J. J. Back,⁵² S. Baker,⁵⁷ V. Balagura,^{9,b} W. Baldini,^{18,44} A. Baranov,³⁹ R. J. Barlow,⁵⁸ S. Barsuk,⁹ W. Barter,⁵⁷ M. Bartolini,²¹ F. Baryshnikov,⁷³ V. Batozskaya,³³ B. Batsukh,⁶³ A. Battig,¹² V. Battista,⁴⁵ A. Bay,⁴⁵ F. Bedeschi,²⁶ I. Bediaga,¹ A. Beiter,⁶³ L. J. Bel,²⁹ S. Belin,²⁴ N. Belyi,⁴ V. Bellec,⁴⁵ N. Belloli,^{22,c} K. Belous,⁴¹ I. Belyaev,³⁶ G. Bencivenni,²⁰ E. Ben-Haim,¹⁰ S. Benson,²⁹ S. Beranek,¹¹ A. Berezhnoy,³⁷ R. Bernet,⁴⁶ D. Berninghoff,¹⁴ E. Bertholet,¹⁰ A. Bertolin,²⁵ C. Betancourt,⁴⁶ F. Betti,^{17,d} M. O. Bettler,⁵¹ Ia. Bezshyiko,⁴⁶ S. Bhasin,⁵⁰ J. Bhom,³¹ M. S. Bieker,¹² S. Bifani,⁴⁹ P. Billoir,¹⁰ A. Birnkraut,¹² A. Bizzeti,^{19,e} M. Björn,⁵⁹ M. P. Blago,⁴⁴ T. Blake,⁵² F. Blanc,⁴⁵ S. Blusk,⁶³ D. Bobulska,⁵⁵ V. Bocci,²⁸ O. Boente Garcia,⁴³ T. Boettcher,⁶⁰ A. Bondar,^{40,f} N. Bondar,³⁵ S. Borghi,^{58,44} M. Borisyak,³⁹ M. Borsato,¹⁴ M. Boubdir,¹¹ T. J. V. Bowcock,⁵⁶ C. Bozzi,^{18,44} S. Braun,¹⁴ M. Brodski,⁴⁴ J. Brodzicka,³¹ A. Brossa Gonzalo,⁵² D. Brundu,^{24,44} E. Buchanan,⁵⁰ A. Buonauro,⁴⁶ C. Burr,⁵⁸ A. Bursche,²⁴ J. S. Butter,²⁹ J. Buytaert,⁴⁴ W. Byczynski,⁴⁴ S. Cadeddu,²⁴ H. Cai,⁶⁷ R. Calabrese,^{18,g} S. Cali,²⁰ R. Calladine,⁴⁹ M. Calvi,^{22,c} M. Calvo Gomez,^{42,h} A. Camboni,^{42,h} P. Campana,²⁰ D. H. Campora Perez,⁴⁴ L. Capriotti,^{17,d} A. Carbone,^{17,d} G. Carboni,²⁷ R. Cardinale,²¹ A. Cardini,²⁴ P. Carniti,^{22,c} K. Carvalho Akiba,² G. Casse,⁵⁶ M. Cattaneo,⁴⁴ G. Cavallero,²¹ R. Cenci,^{26,i} M. G. Chapman,⁵⁰ M. Charles,^{10,44} Ph. Charpentier,⁴⁴ G. Chatzikonstantinidis,⁴⁹ M. Chefdeville,⁶ V. Chekalina,³⁹ C. Chen,³ S. Chen,²⁴ S.-G. Chitic,⁴⁴ V. Chobanova,⁴³ M. Chruszcz,⁴⁴ A. Chubykin,³⁵ P. Ciambone,²⁰ X. Cid Vidal,⁴³ G. Ciezarek,⁴⁴ F. Cindolo,¹⁷ P. E. L. Clarke,⁵⁴ M. Clemencic,⁴⁴ H. V. Cliff,⁵¹ J. Closier,⁴⁴ V. Coco,⁴⁴ J. A. B. Coelho,⁹ J. Cogan,⁸ E. Cogneras,⁷ L. Cojocariu,³⁴ P. Collins,⁴⁴ T. Colombo,⁴⁴ A. Comerma-Montells,¹⁴ A. Contu,²⁴ G. Coombs,⁴⁴ S. Coquereau,⁴² G. Corti,⁴⁴ C. M. Costa Sobral,⁵² B. Couturier,⁴⁴ G. A. Cowan,⁵⁴ D. C. Craik,⁶⁰ A. Crocombe,⁵²

M. Cruz Torres,¹ R. Currie,⁵⁴ C. L. Da Silva,⁷⁸ E. Dall’Occo,²⁹ J. Dalseno,^{43,j} C. D’Ambrosio,⁴⁴ A. Danilina,³⁶ P. d’Argent,¹⁴ A. Davis,⁵⁸ O. De Aguiar Francisco,⁴⁴ K. De Bruyn,⁴⁴ S. De Capua,⁵⁸ M. De Cian,⁴⁵ J. M. De Miranda,¹ L. De Paula,² M. De Serio,^{16,k} P. De Simone,²⁰ J. A. de Vries,²⁹ C. T. Dean,⁵⁵ W. Dean,⁷⁷ D. Decamp,⁶ L. Del Buono,¹⁰ B. Delaney,⁵¹ H.-P. Dembinski,¹³ M. Demmer,¹² A. Dendek,³² D. Derkach,⁷⁴ O. Deschamps,⁷ F. Desse,⁹ F. Dettori,²⁴ B. Dey,⁶⁸ A. Di Canto,⁴⁴ P. Di Nezza,²⁰ S. Didenko,⁷³ H. Dijkstra,⁴⁴ F. Dordei,²⁴ M. Dorigo,^{26,l} A. C. dos Reis,¹ A. Dosil Suárez,⁴³ L. Douglas,⁵⁵ A. Dovbnya,⁴⁷ K. Dreimanis,⁵⁶ L. Dufour,⁴⁴ G. Dujany,¹⁰ P. Durante,⁴⁴ J. M. Durham,⁷⁸ D. Dutta,⁵⁸ R. Dzhelyadin,^{41,a} M. Dziewiecki,¹⁴ A. Dziurda,³¹ A. Dzyuba,³⁵ S. Easo,⁵³ U. Egede,⁵⁷ V. Egorychev,³⁶ S. Eidelman,^{40,f} S. Eisenhardt,⁵⁴ U. Eitschberger,¹² R. Ekelhof,¹² L. Eklund,⁵⁵ S. Ely,⁶³ A. Ene,³⁴ S. Escher,¹¹ S. Esen,²⁹ T. Evans,⁶¹ A. Falabella,¹⁷ C. Färber,⁴⁴ N. Farley,⁴⁹ S. Farry,⁵⁶ D. Fazzini,^{22,c} M. Féo,⁴⁴ P. Fernandez Declara,⁴⁴ A. Fernandez Prieto,⁴³ F. Ferrari,^{17,d} L. Ferreira Lopes,⁴⁵ F. Ferreira Rodrigues,² S. Ferreres Sole,²⁹ M. Ferro-Luzzi,⁴⁴ S. Filippov,³⁸ R. A. Fini,¹⁶ M. Fiorini,^{18,g} M. Firlej,³² C. Fitzpatrick,⁴⁴ T. Fiutowski,³² F. Fleuret,^{9,b} M. Fontana,⁴⁴ F. Fontanelli,^{21,m} R. Forty,⁴⁴ V. Franco Lima,⁵⁶ M. Frank,⁴⁴ C. Frei,⁴⁴ J. Fu,^{23,n} W. Funk,⁴⁴ E. Gabriel,⁵⁴ A. Gallas Torreira,⁴³ D. Galli,^{17,d} S. Gallorini,²⁵ S. Gambetta,⁵⁴ Y. Gan,³ M. Gandelman,² P. Gandini,²³ Y. Gao,³ L. M. Garcia Martin,⁷⁶ J. García Pardiñas,⁴⁶ B. Garcia Plana,⁴³ J. Garra Tico,⁵¹ L. Garrido,⁴² D. Gascon,⁴² C. Gaspar,⁴⁴ G. Gazzoni,⁷ D. Gerick,¹⁴ E. Gersabeck,⁵⁸ M. Gersabeck,⁵⁸ T. Gershon,⁵² D. Gerstel,⁸ Ph. Ghez,⁶ V. Gibson,⁵¹ O. G. Girard,⁴⁵ P. Gironella Gironell,⁴² L. Giubega,³⁴ K. Gizdov,⁵⁴ V. V. Gligorov,¹⁰ C. Göbel,⁶⁵ D. Golubkov,³⁶ A. Golutvin,^{57,73} A. Gomes,^{1,o} I. V. Gorelov,³⁷ C. Gotti,^{22,c} E. Govorkova,²⁹ J. P. Grabowski,¹⁴ R. Graciani Diaz,⁴² L. A. Granado Cardoso,⁴⁴ E. Graugés,⁴² E. Graverini,⁴⁶ G. Graziani,¹⁹ A. Grecu,³⁴ R. Greim,²⁹ P. Griffith,²⁴ L. Grillo,⁵⁸ L. Gruber,⁴⁴ B. R. Gruber Cazon,⁵⁹ C. Gu,³ E. Gushchin,³⁸ A. Guth,¹¹ Yu. Guz,^{41,44} T. Gys,⁴⁴ T. Hadavizadeh,⁵⁹ C. Hadjivasiliou,⁷ G. Haefeli,⁴⁵ C. Haen,⁴⁴ S. C. Haines,⁵¹ P. M. Hamilton,⁶² Q. Han,⁶⁸ X. Han,¹⁴ T. H. Hancock,⁵⁹ S. Hansmann-Menzemer,¹⁴ N. Harnew,⁵⁹ T. Harrison,⁵⁶ C. Hasse,⁴⁴ M. Hatch,⁴⁴ J. He,⁴ M. Hecker,⁵⁷ K. Heinicke,¹² A. Heister,¹² K. Hennessy,⁵⁶ L. Henry,⁷⁶ M. Heß,⁷⁰ J. Heuel,¹¹ A. Hicheur,⁶⁴ R. Hidalgo Charman,⁵⁸ D. Hill,⁵⁹ M. Hilton,⁵⁸ P. H. Hopchev,⁴⁵ J. Hu,¹⁴ W. Hu,⁶⁸ W. Huang,⁴ Z. C. Huard,⁶¹ W. Hulsbergen,²⁹ T. Humair,⁵⁷ M. Hushchyn,⁷⁴ D. Hutchcroft,⁵⁶ D. Hynds,²⁹ P. Ibis,¹² M. Idzik,³² P. Ilten,⁴⁹ A. Inglessi,³⁵ A. Inyakin,⁴¹ K. Ivshin,³⁵ R. Jacobsson,⁴⁴ S. Jakobsen,⁴⁴ J. Jalocha,⁵⁹ E. Jans,²⁹ B. K. Jashal,⁷⁶ A. Jawahery,⁶² F. Jiang,³ M. John,⁵⁹ D. Johnson,⁴⁴ C. R. Jones,⁵¹ C. Joram,⁴⁴ B. Jost,⁴⁴ N. Jurik,⁵⁹ S. Kandybei,⁴⁷ M. Karacson,⁴⁴ J. M. Kariuki,⁵⁰ S. Karodia,⁵⁵ N. Kazeev,⁷⁴ M. Kecke,¹⁴ F. Keizer,⁵¹ M. Kelsey,⁶³ M. Kenzie,⁵¹ T. Ketel,³⁰ B. Khanji,⁴⁴ A. Kharisova,⁷⁵ C. Khurewathanakul,⁴⁵ K. E. Kim,⁶³ T. Kirn,¹¹ V. S. Kirsobom,⁴⁵ S. Klaver,²⁰ K. Klimaszewski,³³ S. Koliiev,⁴⁸ M. Kolpin,¹⁴ R. Kopečna,¹⁴ P. Koppenburg,²⁹ I. Kostiuik,^{29,48} S. Kotriakhova,³⁵ M. Kozeiha,⁷ L. Kravchuk,³⁸ M. Kreps,⁵² F. Kress,⁵⁷ S. Kretzschmar,¹¹ P. Krokovny,^{40,f} W. Krupa,³² W. Krzemien,³³ W. Kucewicz,^{31,p} M. Kucharczyk,³¹ V. Kudryavtsev,^{40,f} G. J. Kunde,⁷⁸ A. K. Kuonen,⁴⁵ T. Kvaratskheliya,³⁶ D. Lacarrere,⁴⁴ G. Lafferty,⁵⁸ A. Lai,²⁴ D. Lancierini,⁴⁶ G. Lanfranchi,²⁰ C. Langenbruch,¹¹ T. Latham,⁵² C. Lazzeroni,⁴⁹ R. Le Gac,⁸ R. Lefèvre,⁷ A. Leflat,³⁷ F. Lemaître,⁴⁴ O. Leroy,⁸ T. Lesiak,³¹ B. Leverington,¹⁴ H. Li,⁶⁶ P.-R. Li,^{4,q} X. Li,⁷⁸ Y. Li,⁵ Z. Li,⁶³ X. Liang,⁶³ T. Likhomanenko,⁷² R. Lindner,⁴⁴ F. Lionetto,⁴⁶ V. Lisovskyi,⁹ G. Liu,⁶⁶ X. Liu,³ D. Loh,⁵² A. Loi,²⁴ I. Longstaff,⁵⁵ J. H. Lopes,² G. Loustau,⁴⁶ G. H. Lovell,⁵¹ D. Lucchesi,^{25,r} M. Lucio Martinez,⁴³ Y. Luo,³ A. Lupato,²⁵ E. Luppi,^{18,g} O. Lupton,⁵² A. Lusiani,²⁶ X. Lyu,⁴ F. Machefert,⁹ F. Maciuc,³⁴ V. Macko,⁴⁵ P. Mackowiak,¹² S. Maddrell-Mander,⁵⁰ O. Maev,^{35,44} K. Maguire,⁵⁸ D. Maisuzenko,³⁵ M. W. Majewski,³² S. Malde,⁵⁹ B. Malecki,⁴⁴ A. Malinin,⁷² T. Maltsev,^{40,f} H. Malygina,¹⁴ G. Manca,^{24,s} G. Mancinelli,⁸ D. Marangotto,^{23,n} J. Maratas,^{7,t} J. F. Marchand,⁶ U. Marconi,¹⁷ C. Marin Benito,⁹ M. Marinangeli,⁴⁵ P. Marino,⁴⁵ J. Marks,¹⁴ P. J. Marshall,⁵⁶ G. Martellotti,²⁸ M. Martinelli,^{44,22,c} D. Martinez Santos,⁴³ F. Martinez Vidal,⁷⁶ A. Massafferri,¹ M. Materok,¹¹ R. Matev,⁴⁴ A. Mathad,⁴⁶ Z. Mathe,⁴⁴ V. Matiunin,³⁶ C. Matteuzzi,²² K. R. Mattioli,⁷⁷ A. Mauri,⁴⁶ E. Maurice,^{9,b} B. Maurin,⁴⁵ M. McCann,^{57,44} A. McNab,⁵⁸ R. McNulty,¹⁵ J. V. Mead,⁵⁶ B. Meadows,⁶¹ C. Meaux,⁸ N. Meinert,⁷⁰ D. Melnychuk,³³ M. Merk,²⁹ A. Merli,^{23,n} E. Michielin,²⁵ D. A. Milanes,⁶⁹ E. Millard,⁵² M.-N. Minard,⁶ O. Mineev,³⁶ L. Minzoni,^{18,g} D. S. Mitzel,¹⁴ A. Mödden,¹² A. Mogini,¹⁰ R. D. Moise,⁵⁷ T. Mombächer,¹² I. A. Monroy,⁶⁹ S. Monteil,⁷ M. Morandin,²⁵ G. Morello,²⁰ M. J. Morello,^{26,u} J. Moron,³² A. B. Morris,⁸ R. Mountain,⁶³ F. Muheim,⁵⁴ M. Mukherjee,⁶⁸ M. Mulder,²⁹ D. Müller,⁴⁴ J. Müller,¹² K. Müller,⁴⁶ V. Müller,¹² C. H. Murphy,⁵⁹ D. Murray,⁵⁸ P. Naik,⁵⁰ T. Nakada,⁴⁵ R. Nandakumar,⁵³ A. Nandi,⁵⁹ T. Nanut,⁴⁵ I. Nasteva,² M. Needham,⁵⁴ N. Neri,^{23,n} S. Neubert,¹⁴ N. Neufeld,⁴⁴ R. Newcombe,⁵⁷ T. D. Nguyen,⁴⁵ C. Nguyen-Mau,^{45,v} S. Nieswand,¹¹ R. Niet,¹² N. Nikitin,³⁷ N. S. Nolte,⁴⁴ A. Oblakowska-Mucha,³² V. Obraztsov,⁴¹ S. Ogilvy,⁵⁵ D. P. O’Hanlon,¹⁷ R. Oldeman,^{24,s} C. J. G. Onderwater,⁷¹ J. D. Osborn,⁷⁷ A. Ossowska,³¹ J. M. Otalora Goicochea,² T. Ovsiannikova,³⁶ P. Owen,⁴⁶ A. Oyanguren,⁷⁶ P. R. Pais,⁴⁵ T. Pajero,^{26,u} A. Palano,¹⁶ M. Palutan,²⁰ G. Panshin,⁷⁵ A. Papanestis,⁵³ M. Pappagallo,⁵⁴ L. L. Pappalardo,^{18,g} W. Parker,⁶²

C. Parkes,^{58,44} G. Passaleva,^{19,44} A. Pastore,¹⁶ M. Patel,⁵⁷ C. Patrignani,^{17,d} A. Pearce,⁴⁴ A. Pellegrino,²⁹ G. Penso,²⁸ M. Pepe Altarelli,⁴⁴ S. Perazzini,¹⁷ D. Pereima,³⁶ P. Perret,⁷ L. Pescatore,⁴⁵ K. Petridis,⁵⁰ A. Petrolini,^{21,m} A. Petrov,⁷² S. Petrucci,⁵⁴ M. Petruzzo,^{23,n} B. Pietrzyk,⁶ G. Pietrzyk,⁴⁵ M. Pikiés,³¹ M. Pili,⁵⁹ D. Pinci,²⁸ J. Pinzino,⁴⁴ F. Pisani,⁴⁴ A. Piucci,¹⁴ V. Placinta,³⁴ S. Playfer,⁵⁴ J. Plews,⁴⁹ M. Plo Casasus,⁴³ F. Polci,¹⁰ M. Poli Lener,²⁰ M. Poliakov,⁶³ A. Poluektov,⁸ N. Polukhina,^{73,w} I. Polyakov,⁶³ E. Polycarpo,² G. J. Pomery,⁵⁰ S. Ponce,⁴⁴ A. Popov,⁴¹ D. Popov,^{49,13} S. Poslavskii,⁴¹ E. Price,⁵⁰ C. Prouve,⁴³ V. Pugatch,⁴⁸ A. Puig Navarro,⁴⁶ H. Pullen,⁵⁹ G. Punzi,^{26,i} W. Qian,⁴ J. Qin,⁴ R. Quagliani,¹⁰ B. Quintana,⁷ N. V. Raab,¹⁵ B. Rachwal,³² J. H. Rademacker,⁵⁰ M. Rama,²⁶ M. Ramos Pernas,⁴³ M. S. Rangel,² F. Ratnikov,^{39,74} G. Raven,³⁰ M. Ravonel Salzgeber,⁴⁴ M. Reboud,⁶ F. Redi,⁴⁵ S. Reichert,¹² F. Reiss,¹⁰ C. Remon Alepuz,⁷⁶ Z. Ren,³ V. Renaudin,⁵⁹ S. Ricciardi,⁵³ S. Richards,⁵⁰ K. Rinnert,⁵⁶ P. Robbe,⁹ A. Robert,¹⁰ A. B. Rodrigues,⁴⁵ E. Rodrigues,⁶¹ J. A. Rodriguez Lopez,⁶⁹ M. Roehrken,⁴⁴ S. Roiser,⁴⁴ A. Rollings,⁵⁹ V. Romanovskiy,⁴¹ A. Romero Vidal,⁴³ J. D. Roth,⁷⁷ M. Rotondo,²⁰ M. S. Rudolph,⁶³ T. Ruf,⁴⁴ J. Ruiz Vidal,⁷⁶ J. J. Saborido Silva,⁴³ N. Sagidova,³⁵ B. Saitta,^{24,s} V. Salustino Guimaraes,⁶⁵ C. Sanchez Gras,²⁹ C. Sanchez Mayordomo,⁷⁶ B. Sanmartin Sedes,⁴³ R. Santacesaria,²⁸ C. Santamarina Rios,⁴³ M. Santimaria,^{20,44} E. Santovetti,^{27,x} G. Sarpis,⁵⁸ A. Sarti,^{20,y} C. Satriano,^{28,z} A. Satta,²⁷ M. Saur,⁴ D. Savrina,^{36,37} S. Schael,¹¹ M. Schellenberg,¹² M. Schiller,⁵⁵ H. Schindler,⁴⁴ M. Schmelling,¹³ T. Schmelzer,¹² B. Schmidt,⁴⁴ O. Schneider,⁴⁵ A. Schopper,⁴⁴ H. F. Schreiner,⁶¹ M. Schubiger,⁴⁵ S. Schulte,⁴⁵ M. H. Schune,⁹ R. Schwemmer,⁴⁴ B. Sciascia,²⁰ A. Sciubba,^{28,y} A. Semennikov,³⁶ E. S. Sepulveda,¹⁰ A. Sergi,^{49,44} N. Serra,⁴⁶ J. Serrano,⁸ L. Sestini,²⁵ A. Seuthe,¹² P. Seyfert,⁴⁴ M. Shapkin,⁴¹ T. Shears,⁵⁶ L. Shekhtman,^{40,f} V. Shevchenko,⁷² E. Shmanin,⁷³ B. G. Siddi,¹⁸ R. Silva Coutinho,⁴⁶ L. Silva de Oliveira,² G. Simi,^{25,r} S. Simone,^{16,k} I. Skiba,¹⁸ N. Skidmore,¹⁴ T. Skwarnicki,⁶³ M. W. Slater,⁴⁹ J. G. Smeaton,⁵¹ E. Smith,¹¹ I. T. Smith,⁵⁴ M. Smith,⁵⁷ M. Soares,¹⁷ I. Soares Lavra,¹ M. D. Sokoloff,⁶¹ F. J. P. Soler,⁵⁵ B. Souza De Paula,² B. Spaan,¹² E. Spadaro Norella,^{23,n} P. Spradlin,⁵⁵ F. Stagni,⁴⁴ M. Stahl,¹⁴ S. Stahl,⁴⁴ P. Stefko,⁴⁵ S. Stefkova,⁵⁷ O. Steinkamp,⁴⁶ S. Stemmler,¹⁴ O. Stenyakin,⁴¹ M. Stepanova,³⁵ H. Stevens,¹² A. Stocchi,⁹ S. Stone,⁶³ S. Stracka,²⁶ M. E. Stramaglia,⁴⁵ M. Straticiuc,³⁴ U. Straumann,⁴⁶ S. Strovkov,⁷⁵ J. Sun,³ L. Sun,⁶⁷ Y. Sun,⁶² K. Swientek,³² A. Szabelski,³³ T. Szumlak,³² M. Szymanski,⁴ Z. Tang,³ T. Tekampe,¹² G. Tellarini,¹⁸ F. Teubert,⁴⁴ E. Thomas,⁴⁴ M. J. Tilley,⁵⁷ V. Tisserand,⁷ S. T'Jampens,⁶ M. Tobin,⁵ S. Tolk,⁴⁴ L. Tomassetti,^{18,g} D. Tonelli,²⁶ D. Y. Tou,¹⁰ R. Tourinho Jadallah Aoude,¹ E. Tournefier,⁶ M. Traill,⁵⁵ M. T. Tran,⁴⁵ A. Trisovic,⁵¹ A. Tsaregorodtsev,⁸ G. Tuci,^{26,44,i} A. Tully,⁵¹ N. Tuning,²⁹ A. Ukleja,³³ A. Usachov,⁹ A. Ustyuzhanin,^{39,74} U. Uwer,¹⁴ A. Vagner,⁷⁵ V. Vagnoni,¹⁷ A. Valassi,⁴⁴ S. Valat,⁴⁴ G. Valenti,¹⁷ M. van Beuzekom,²⁹ H. Van Hecke,⁷⁸ E. van Herwijnen,⁴⁴ C. B. Van Hulse,¹⁵ J. van Tilburg,²⁹ M. van Veghel,²⁹ R. Vazquez Gomez,⁴⁴ P. Vazquez Regueiro,⁴³ C. Vázquez Sierra,²⁹ S. Vecchi,¹⁸ J. J. Velthuis,⁵⁰ M. Veltri,^{19,aa} A. Venkateswaran,⁶³ M. Vernet,⁷ M. Veronesi,²⁹ M. Vesterinen,⁵² J. V. Viana Barbosa,⁴⁴ D. Vieira,⁴ M. Vieites Diaz,⁴³ H. Viemann,⁷⁰ X. Vilasis-Cardona,^{42,h} A. Vitkovskiy,²⁹ M. Vitti,⁵¹ V. Volkov,³⁷ A. Vollhardt,⁴⁶ D. Vom Bruch,¹⁰ B. Voneki,⁴⁴ A. Vorobyev,³⁵ V. Vorobyev,^{40,f} N. Voropaev,³⁵ R. Waldi,⁷⁰ J. Walsh,²⁶ J. Wang,⁵ M. Wang,³ Y. Wang,⁶⁸ Z. Wang,⁴⁶ D. R. Ward,⁵¹ H. M. Wark,⁵⁶ N. K. Watson,⁴⁹ D. Websdale,⁵⁷ A. Weiden,⁴⁶ C. Weisser,⁶⁰ M. Whitehead,¹¹ G. Wilkinson,⁵⁹ M. Wilkinson,⁶³ I. Williams,⁵¹ M. Williams,⁶⁰ M. R. J. Williams,⁵⁸ T. Williams,⁴⁹ F. F. Wilson,⁵³ M. Winn,⁹ W. Wislicki,³³ M. Witek,³¹ G. Wormser,⁹ S. A. Wotton,⁵¹ K. Wyllie,⁴⁴ D. Xiao,⁶⁸ Y. Xie,⁶⁸ H. Xing,⁶⁶ A. Xu,³ M. Xu,⁶⁸ Q. Xu,⁴ Z. Xu,⁶ Z. Xu,³ Z. Yang,³ Z. Yang,⁶² Y. Yao,⁶³ L. E. Yeomans,⁵⁶ H. Yin,⁶⁸ J. Yu,^{68,bb} X. Yuan,⁶³ O. Yushchenko,⁴¹ K. A. Zarebski,⁴⁹ M. Zavertyaev,^{13,w} M. Zeng,³ D. Zhang,⁶⁸ L. Zhang,³ W. C. Zhang,^{3,cc} Y. Zhang,⁴⁴ A. Zhelezov,¹⁴ Y. Zheng,⁴ X. Zhu,³ V. Zhukov,^{11,37} J. B. Zonneveld,⁵⁴ and S. Zucchelli^{17,d}

(LHCb Collaboration)

¹Centro Brasileiro de Pesquisas Físicas (CBPF), Rio de Janeiro, Brazil

²Universidade Federal do Rio de Janeiro (UFRJ), Rio de Janeiro, Brazil

³Center for High Energy Physics, Tsinghua University, Beijing, China

⁴University of Chinese Academy of Sciences, Beijing, China

⁵Institute Of High Energy Physics (ihep), Beijing, China

⁶Univ. Grenoble Alpes, Univ. Savoie Mont Blanc, CNRS, IN2P3-LAPP, Annecy, France

⁷Université Clermont Auvergne, CNRS/IN2P3, LPC, Clermont-Ferrand, France

⁸Aix Marseille Univ, CNRS/IN2P3, CPPM, Marseille, France

⁹LAL, Univ. Paris-Sud, CNRS/IN2P3, Université Paris-Saclay, Orsay, France

¹⁰LPNHE, Sorbonne Université, Paris Diderot Sorbonne Paris Cité, CNRS/IN2P3, Paris, France

- ¹¹*I. Physikalisches Institut, RWTH Aachen University, Aachen, Germany*
¹²*Fakultät Physik, Technische Universität Dortmund, Dortmund, Germany*
¹³*Max-Planck-Institut für Kernphysik (MPIK), Heidelberg, Germany*
¹⁴*Physikalisches Institut, Ruprecht-Karls-Universität Heidelberg, Heidelberg, Germany*
¹⁵*School of Physics, University College Dublin, Dublin, Ireland*
¹⁶*INFN Sezione di Bari, Bari, Italy*
¹⁷*INFN Sezione di Bologna, Bologna, Italy*
¹⁸*INFN Sezione di Ferrara, Ferrara, Italy*
¹⁹*INFN Sezione di Firenze, Firenze, Italy*
²⁰*INFN Laboratori Nazionali di Frascati, Frascati, Italy*
²¹*INFN Sezione di Genova, Genova, Italy*
²²*INFN Sezione di Milano-Bicocca, Milano, Italy*
²³*INFN Sezione di Milano, Milano, Italy*
²⁴*INFN Sezione di Cagliari, Monserrato, Italy*
²⁵*INFN Sezione di Padova, Padova, Italy*
²⁶*INFN Sezione di Pisa, Pisa, Italy*
²⁷*INFN Sezione di Roma Tor Vergata, Roma, Italy*
²⁸*INFN Sezione di Roma La Sapienza, Roma, Italy*
²⁹*Nikhef National Institute for Subatomic Physics, Amsterdam, Netherlands*
³⁰*Nikhef National Institute for Subatomic Physics and VU University Amsterdam, Amsterdam, Netherlands*
³¹*Henryk Niewodniczanski Institute of Nuclear Physics Polish Academy of Sciences, Kraków, Poland*
³²*AGH—University of Science and Technology, Faculty of Physics and Applied Computer Science, Kraków, Poland*
³³*National Center for Nuclear Research (NCBJ), Warsaw, Poland*
³⁴*Horia Hulubei National Institute of Physics and Nuclear Engineering, Bucharest-Magurele, Romania*
³⁵*Petersburg Nuclear Physics Institute NRC Kurchatov Institute (PNPI NRC KI), Gatchina, Russia*
³⁶*Institute of Theoretical and Experimental Physics NRC Kurchatov Institute (ITEP NRC KI), Moscow, Russia, Moscow, Russia*
³⁷*Institute of Nuclear Physics, Moscow State University (SINP MSU), Moscow, Russia*
³⁸*Institute for Nuclear Research of the Russian Academy of Sciences (INR RAS), Moscow, Russia*
³⁹*Yandex School of Data Analysis, Moscow, Russia*
⁴⁰*Budker Institute of Nuclear Physics (SB RAS), Novosibirsk, Russia*
⁴¹*Institute for High Energy Physics NRC Kurchatov Institute (IHEP NRC KI), Protvino, Russia, Protvino, Russia*
⁴²*ICCUB, Universitat de Barcelona, Barcelona, Spain*
⁴³*Instituto Galego de Física de Altas Enerxías (IGFAE), Universidade de Santiago de Compostela, Santiago de Compostela, Spain*
⁴⁴*European Organization for Nuclear Research (CERN), Geneva, Switzerland*
⁴⁵*Institute of Physics, Ecole Polytechnique Fédérale de Lausanne (EPFL), Lausanne, Switzerland*
⁴⁶*Physik-Institut, Universität Zürich, Zürich, Switzerland*
⁴⁷*NSC Kharkiv Institute of Physics and Technology (NSC KIPT), Kharkiv, Ukraine*
⁴⁸*Institute for Nuclear Research of the National Academy of Sciences (KINR), Kyiv, Ukraine*
⁴⁹*University of Birmingham, Birmingham, United Kingdom*
⁵⁰*H.H. Wills Physics Laboratory, University of Bristol, Bristol, United Kingdom*
⁵¹*Cavendish Laboratory, University of Cambridge, Cambridge, United Kingdom*
⁵²*Department of Physics, University of Warwick, Coventry, United Kingdom*
⁵³*STFC Rutherford Appleton Laboratory, Didcot, United Kingdom*
⁵⁴*School of Physics and Astronomy, University of Edinburgh, Edinburgh, United Kingdom*
⁵⁵*School of Physics and Astronomy, University of Glasgow, Glasgow, United Kingdom*
⁵⁶*Oliver Lodge Laboratory, University of Liverpool, Liverpool, United Kingdom*
⁵⁷*Imperial College London, London, United Kingdom*
⁵⁸*School of Physics and Astronomy, University of Manchester, Manchester, United Kingdom*
⁵⁹*Department of Physics, University of Oxford, Oxford, United Kingdom*
⁶⁰*Massachusetts Institute of Technology, Cambridge, Massachusetts, USA*
⁶¹*University of Cincinnati, Cincinnati, Ohio, USA*
⁶²*University of Maryland, College Park, Maryland, USA*
⁶³*Syracuse University, Syracuse, New York, USA*
⁶⁴*Laboratory of Mathematical and Subatomic Physics, Constantine, Algeria*
[associated with Universidade Federal do Rio de Janeiro (UFRJ), Rio de Janeiro, Brazil]

⁶⁵*Pontifícia Universidade Católica do Rio de Janeiro (PUC-Rio), Rio de Janeiro, Brazil
[associated with Universidade Federal do Rio de Janeiro (UFRJ), Rio de Janeiro, Brazil]*

⁶⁶*South China Normal University, Guangzhou, China
(associated with Center for High Energy Physics, Tsinghua University, Beijing, China)*

⁶⁷*School of Physics and Technology, Wuhan University, Wuhan, China
(associated with Center for High Energy Physics, Tsinghua University, Beijing, China)*

⁶⁸*Institute of Particle Physics, Central China Normal University, Wuhan, Hubei, China
(associated with Center for High Energy Physics, Tsinghua University, Beijing, China)*

⁶⁹*Departamento de Física, Universidad Nacional de Colombia, Bogota, Colombia
(associated with LPNHE, Sorbonne Université, Paris Diderot Sorbonne Paris Cité,
CNRS/IN2P3, Paris, France)*

⁷⁰*Institut für Physik, Universität Rostock, Rostock, Germany
(associated with Physikalisches Institut, Ruprecht-Karls-Universität Heidelberg, Heidelberg, Germany)*

⁷¹*Van Swinderen Institute, University of Groningen, Groningen, Netherlands
(associated with Nikhef National Institute for Subatomic Physics, Amsterdam, Netherlands)*

⁷²*National Research Centre Kurchatov Institute, Moscow, Russia [associated with Institute of Theoretical
and Experimental Physics NRC Kurchatov Institute (ITEP NRC KI), Moscow, Russia]*

⁷³*National University of Science and Technology “MISIS”, Moscow, Russia [associated with Institute of
Theoretical and Experimental Physics NRC Kurchatov Institute (ITEP NRC KI), Moscow, Russia]*

⁷⁴*National Research University Higher School of Economics, Moscow, Russia
(associated with Yandex School of Data Analysis, Moscow, Russia)*

⁷⁵*National Research Tomsk Polytechnic University, Tomsk, Russia [associated with Institute of Theoretical
and Experimental Physics NRC Kurchatov Institute (ITEP NRC KI), Moscow, Russia]*

⁷⁶*Instituto de Física Corpuscular, Centro Mixto Universidad de Valencia - CSIC, Valencia, Spain
(associated with ICCUB, Universitat de Barcelona, Barcelona, Spain)*

⁷⁷*University of Michigan, Ann Arbor, USA
(associated with Syracuse University, Syracuse, New York, USA)*

⁷⁸*Los Alamos National Laboratory (LANL), Los Alamos, USA
(associated with Syracuse University, Syracuse, New York, USA)*

^aDeceased.

^bAlso at Laboratoire Leprince-Ringuet, Palaiseau, France.

^cAlso at Università di Milano Bicocca, Milano, Italy.

^dAlso at Università di Bologna, Bologna, Italy.

^eAlso at Università di Modena e Reggio Emilia, Modena, Italy.

^fAlso at Novosibirsk State University, Novosibirsk, Russia.

^gAlso at Università di Ferrara, Ferrara, Italy.

^hAlso at LIFAELS, La Salle, Universitat Ramon Llull, Barcelona, Spain.

ⁱAlso at Università di Pisa, Pisa, Italy.

^jAlso at H.H. Wills Physics Laboratory, University of Bristol, Bristol, United Kingdom.

^kAlso at Università di Bari, Bari, Italy.

^lAlso at Sezione INFN di Trieste, Trieste, Italy.

^mAlso at Università di Genova, Genova, Italy.

ⁿAlso at Università degli Studi di Milano, Milano, Italy.

^oAlso at Universidade Federal do Triângulo Mineiro (UFMG), Uberaba-MG, Brazil.

^pAlso at AGH - University of Science and Technology, Faculty of Computer Science, Electronics and Telecommunications, Kraków, Poland.

^qAlso at Lanzhou University, Lanzhou, China.

^rAlso at Università di Padova, Padova, Italy.

^sAlso at Università di Cagliari, Cagliari, Italy.

^tAlso at MSU - Iligan Institute of Technology (MSU-IIT), Iligan, Philippines.

^uAlso at Scuola Normale Superiore, Pisa, Italy.

^vAlso at Hanoi University of Science, Hanoi, Vietnam.

^wAlso at P.N. Lebedev Physical Institute, Russian Academy of Science (LPI RAS), Moscow, Russia.

^xAlso at Università di Roma Tor Vergata, Roma, Italy.

^yAlso at Università di Roma La Sapienza, Roma, Italy.

^zAlso at Università della Basilicata, Potenza, Italy.

^{aa}Also at Università di Urbino, Urbino, Italy.

^{bb}Also at Physics and Micro Electronic College, Hunan University, Changsha City, China.

^{cc}Also at School of Physics and Information Technology, Shaanxi Normal University (SNNU), Xi'an, China.